



# Conductivity mapping of topographically complex surfaces using contact-mode carbon fibre in potentiometric SECM

Rabea Saleh Rabea Bin Sowad<sup>a</sup>, László Kiss<sup>b,c</sup>, András Kiss<sup>a,\*</sup>

<sup>a</sup> Department of Physical Chemistry and Materials Science, Faculty of Sciences, University of Pécs, Ifjúság útja 6, 7624 Pécs, Hungary

<sup>b</sup> Department of Organic and Medicinal Chemistry, Medical School, University of Pécs, Honvéd utca 1, 7624 Pécs, Hungary

<sup>c</sup> János Szentágothai Research Centre, University of Pécs, Ifjúság útja 20, 7624 Pécs, Hungary

## ARTICLE INFO

### Keywords:

Scanning electrochemical microscopy (SECM)  
Potentiometry  
Topography

## ABSTRACT

In numerous scientific and engineering applications, it is imperative to study the reactivity of material surfaces at a microscopic level. Scanning electrochemical microscopy (SECM) is a prevalent technique utilized to investigate and probe the electrochemical properties of surfaces. However, due to the inherent dependence of SECM on the distance between the sample and tip, uneven samples can pose a challenge, resulting in inaccurate measurements and incomplete understanding of material behavior. In this paper, we propose a novel approach for resolving this issue using contact-mode carbon fiber electrodes in potentiometric mode. The methodology introduced in this study presents a progressive development over the conventional feedback mode in certain circumstances, as it is capable of monitoring sample conductivity independent of its topography. This paper exemplifies two specific cases involving a tilted and a rough surface. A comparative analysis of the results obtained using the conventional feedback mode and the proposed method was conducted to further validate its efficacy. The findings demonstrate that the proposed method is highly effective in studying tilted and rugged substrates.

## 1. Introduction

Scanning electrochemical microscopy (SECM) is a powerful technique used to study surface reactivity at a microscopic level. SECM has several modes of operation, with feedback mode being the most widely used. This mode utilizes a disk-shaped ultramicroelectrode (UME) whose tip current decreases when it is close to an insulating target due to hindered diffusion of electroactive species towards its sensing disk (negative feedback). Conversely, when the UME tip is in close proximity to a conductive surface, electron transfer between the mediator and the surface is facilitated, regenerating consumed redox species and increasing the tip current (positive feedback) [1,2]. In SECM experiments, constant height mode is commonly employed, where an approach curve is first performed to position the UME tip at the appropriate working distance where feedback effects take place. The effect of the feedback can then be used to image the topography and regional differences in the conductivity of the sample surface. The electrochemical signals, however, are often very sensitive to tip-sample separation. On samples with an intricate surface topography, the resulting current map is a superposition of electrochemical activity and topography [1].

Another long-standing issue in the implementation of SECM is the risk of tip collision when it is scanned at constant-height along a tilted surface or when the height of the 3D structures on the sample surface is substantially larger than the diameter of the SECM tip itself [3]. Moreover, the feedback or collection efficiency is compromised if the tip is scanned away from a tilted surface or during scanning above grooves or holes which makes the application of this technique limited for samples that are both electrochemically and topographically heterogeneous [4]. Since the changes in the tip response caused by the tip-distance variations cannot be distinguished from those resulting from the changes in conductivity, further specifics of the specimen's morphology are essential in order to allow for a deconvolution of these two components.

Various techniques to regulate the tip-sample distance or map topography and surface reactivity simultaneously have been proposed, including shear force detection [5,6], electrochemical probe integration into AFM [7,8], SICM [9,10], AC-SECM [11,12], and tip position modulation [13]. However, these techniques suffer from various limitations such as poor performance with soft samples [14], complicated instrumentation [15], and the requirement of special electrode design [16] or sample cells [17]. Soft probes such as stylus soft probes [18] and soft linear microelectrode arrays [19] have been developed for imaging 3D

\* Corresponding author.

E-mail addresses: [mce6bg@tr.pte.hu](mailto:mce6bg@tr.pte.hu) (R.S.R.B. Sowad), [kissl@gamma.ttk.pte.hu](mailto:kissl@gamma.ttk.pte.hu) (L. Kiss), [akiss@gamma.ttk.pte.hu](mailto:akiss@gamma.ttk.pte.hu) (A. Kiss).

or tilted surfaces in a brushing-like motion in amperometric mode. However, these probes have limitations, including reduced resolution due to changes in contact angle or polymer coating thickness causing an increase in probe-sample distance [3] or inability to penetrate small surface corrugations [20]. These limitations can result in an increased working distance, allowing topographic features to be measured.

This paper aims to obtain images that are unimpaired by topography convolution when using SECM, and the tip response can only be attributed to the activity of the sample. The approach proposed in this work is to scan the surface under investigation in contact mode with carbon fibre. A similar approach, named ‘nanopotentiometry’ [21] has been used before to study the  $I$ - $V$  characteristics of metal-oxide semiconductor transistors where the potential difference between an AFM tip and the transistor was mapped, while the two were in direct contact. In this work the potential difference between the carbon fibre and the sample being inspected was monitored without the use of a reference electrode. In the case of direct contact between the conductive sample and carbon fibre, there is zero potential difference. In any other scenario, the electrochemical nature of the solution surrounding the sample determines the non-zero potential (Fig. 1). This proposed technique was performed on two different samples – a tilted sample and a controlled-cut sample – and compared to the conventional feedback mode.

## 2. Materials and methods

### 2.1. Ultramicroelectrodes (UME)

Two types of electrodes were prepared. A disk-shaped platinum ultramicroelectrode that was used for the conventional measurement in feedback mode. To fabricate the Pt electrode, a borosilicate glass from World Precision Instrument (WPI) with a 1 mm inner diameter and 2 mm outer diameter was heated and sealed from one end. A Goodfellow Cambridge hard-tempered 25  $\mu\text{m}$ -diameter Pt wire with 99.9 % purity and a length of less than 1 cm was inserted into the capillary glass. The borosilicate glass was then heated again to seal it around the Pt wire. To expose the electroactive surface of the Pt electrode, the electrode was treated with coarse P60 abrasive sandpaper and subsequently polished with a 4000-grit polisher.

The other UME is a carbon fiber electrode that was utilized for the potentiometric measurement of the proposed technique. To fabricate the electrode, a borosilicate glass with a 1 mm inner diameter and 2 mm outer diameter was half-sealed from one end. A conducting silver paste (Amepox Micro-electronics, Ltd. 90-268 Lodz Jaracza, Poland) was applied to one end of an electric wire and connected to a 1–1.5 cm long carbon fiber strand of a 7  $\mu\text{m}$  diameter. The wire was left to cure for 24 h and inspected under a microscope to ensure that only one strand was

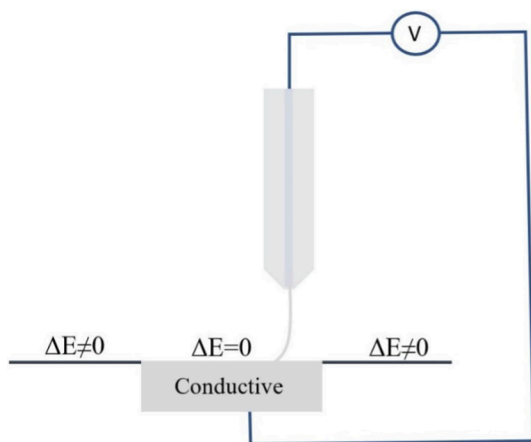


Fig. 1. A diagram depicting the proposed potentiometric contact-mode set-up with the potential difference observed at different regions of the sample.

properly connected. Careful insertion of the electric wire under the microscope into the borosilicate glass was then performed, leaving about 0.5 cm of the carbon fiber strand protruding from one end of the glass.

### 2.2. Targets

To create the model targets, two samples were molded using Epofix (Struers, Ballerup, Denmark) resin. The mold was made using a piece of a Falcon-tube that was cut off, and then 1 mm-diameter platinum samples were inserted upside-down into the prepared mold and connected to crocodile clips. Epofix resin was poured into the mold and allowed to cure. Once cured, the surfaces of the samples were exposed by polishing with P60 and 4000-grit sandpapers, and the surface was cleaned and degreased using absolute ethanol. Finally, a controlled cut was made on top of one of the target (Fig. 2).

### 2.3. SECM instrumentation

A Homemade SECM instrument was used to conduct the measurement. The control (positioning) unit and the electrochemical measurement unit are the two principal components of the system. The relative position of the target and the measurement tip was adjusted by the positioning system which was designed using an Eppendorf 3030 Heka MIM4 motorized 3-axis micromanipulator (Eppendorf AG, Hamburg, Germany). The SECM stand and sample holder, which allows for precise manual positioning and leveling, was made from an old optical microscope and a mirror holder. The measuring instrument was a programmable 4-channel eDAQ ISOPOD 452 (eDAQ Pty Ltd., Australia) data acquisition device with high impedance input to measure the potential against an Hg/Hg<sub>2</sub>Cl<sub>2</sub>/3M KCl reference electrode. The whole system was controlled by a set of Bash scripts in a linux terminal which integrates and governs motions, data gathering, and data correction.

### 2.4. Measurement approach

For the feedback mode, a Pt electrode was used to measure the potential against a calomel electrode [Hg/Hg<sub>2</sub>Cl<sub>2</sub>/3M KCl] as a reference electrode. 10 mM K<sub>3</sub>[Fe(CN)<sub>6</sub>] redox mediator in 0.1 M KCl that served as a background electrolyte were used. An approach curve was first performed, and the Z-distance was established to be 50  $\mu\text{m}$  at which the positive and negative feedback effects can be distinguished. 2D scans were carried out above the targets at a constant height to obtain a current image of the surface (amperometric measurement).

The proposed method used fabricated carbon fibre electrodes in 10 mM K<sub>3</sub>[Fe(CN)<sub>6</sub>] redox mediator and 0.1 M KCl background electrolyte without the requirement of a reference electrode. One input of the high impedance voltmeter was connected to the indicator electrode (carbon fibre) and the other to the conductive part of the target (Pt) which acts as a reference electrode. Through a downward gradual approach with 1  $\mu\text{m}$  step size, the carbon fibre was brought into close proximity with the conductive element. Upon observing a sudden transition in potential from an open circuit to zero, it was evident that the carbon fibre contacted the surface. In order to allow for the bending of the carbon fibre, an additional 500  $\mu\text{m}$  downward-shift was introduced. Throughout the entire experiment, the carbon fibre strand was kept in contact with the target. A fast comb scanning algorithm [22] was then carried out to produce the desired potential map (potentiometric measurement).

Fig. 3 exhibits two distinct scenarios, with the first case indicating the absence of physical contact between the carbon fiber and the conductive region of the substrate (Fig. 3a). In this instance, the potential difference is non-zero, which can be attributed to the potential difference of the electrochemical cell described by Eq. (1):



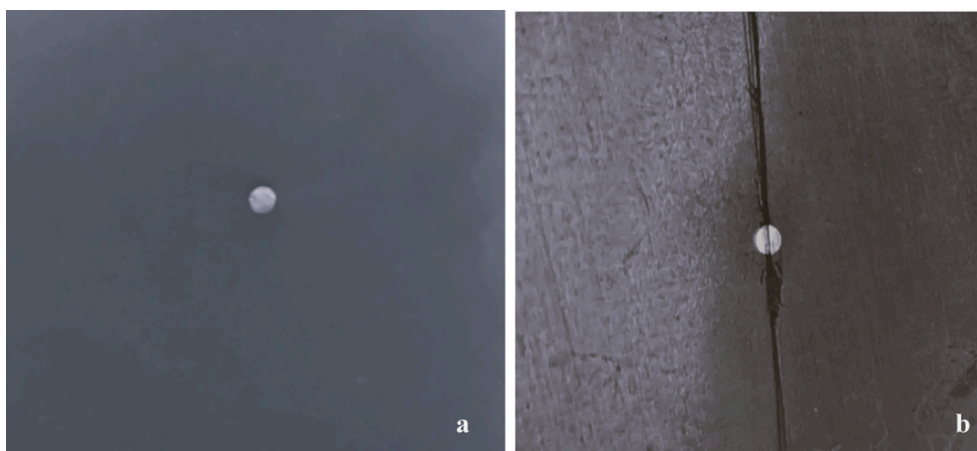


Fig. 2. Optical images of (a) a smooth substrate that was utilized as a tilted sample, (b) a controlled-cut target that was employed as a rugged sample.

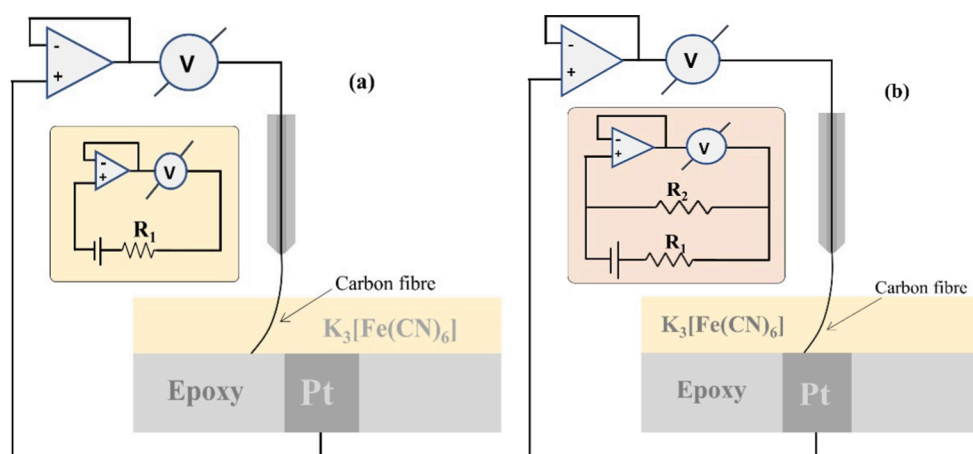


Fig. 3. Measurement approach of the proposed potentiometric contact-mode in cases of (a) no contact between the carbon fibre electrode and the Pt substrate, (b) a direct physical contact between the carbon fibre and the Pt substrate.

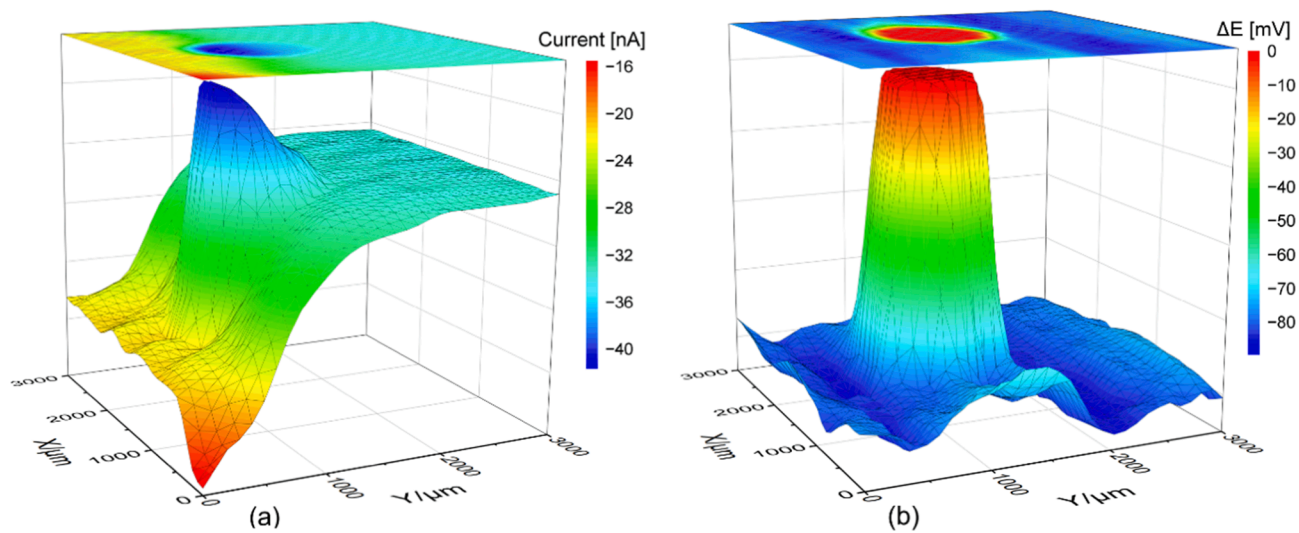


Fig. 4. 3D images of the tilted target obtained by (a) Feedback mode using Pt disk-shaped UME. Current was measured against an  $Hg/Hg_2Cl_2/3M$  KCl reference electrode. Step size was 100  $\mu m$  on both axes for the Cartesian coordinate-based images. (b) Potentiometric contact-mode using carbon fibre UME. Step size was 100  $\mu m$  on both axes.

Fig. 3b shows the case where a direct physical contact between the carbon fiber and the active region of the target material is established. This forms a voltage divider between the potentiometer and the system under investigation, with  $R_1$  and  $R_2$  representing the resistances between the carbon fiber and the conductive substrate through the electrolyte and when in direct contact, respectively.

### 3. Results and discussion

#### 3.1. Tilted target

For this experiment, a smooth substrate (Fig. 2a) was used with an almost 2-degree y-axis angle tilt. The expected outcome of the feedback mode experiment would be an increase in current flow above the passive region and a decrease in current flow above the active area as the probe progresses along y-axis. The experiment's results confirmed this expectation where a considerable difference in the measured current flow of approximately 25–15nA was observed between the conductive and inert regions in one half of the target (Fig. 4a). However, towards the end of the other half of the Pt substrate, it became exceedingly difficult to differentiate between the two zones, as the contrast diminished, with the measured signals being nearly identical over the two sections. In situations where the morphology of the substrate is not a priori understood, discriminating between the contributions of electrochemical and topographical factors to the observed variations in the target's activity presents a challenge [5]. As for the potentiometric contact-mode approach, the images gathered confirmed that the effect observed in the feedback mode was not exclusively induced by the sample's activity but rather a combination of its activity and topography. The results indicated that the potential difference over the active section of the tilted target was 0 mV, while  $-80$  mV elsewhere on the sample (Fig. 4b). Notably, the measurements remained uniform above the active target, irrespective of the sample's tilt. It is worth mentioning that one advantage of utilizing feedback mode is its ability to visualize alterations in electrochemical activity under positive feedback conditions. However, in the absence of distance control, this can potentially result in incorrect interpretations if the structure of the surface is unknown. Although the proposed contact-mode approach offers less information about the activity, it serves as a valuable complementary method in distinguishing between conducting and non-conducting regions of complex topographies.

#### 3.2. Controlled-cut target

15. In the case of the cut-target (Fig. 2b), the topography effect of the cut can be visibly seen as the current on top of the passive and active zones above the slit falls within the same range of 120–140nA (Fig. 5a). For the proposed potentiometric contact-mode approach, the potential difference above the active zone was 0 mV and around  $-160$  mV on the inactive region (Fig. 5b). A distinctive characteristic of this potentiometric mode resides in its capacity to maintain a constant concentration of the analyte species throughout the entirety of the measurement process, due to the absence of faradaic reactions which ensures that the local potential measured is typically linearly correlated with the activity of the analyte [23]. The composition of the solution, carbon fibre and the target present the main source of the non-zero potential difference of the electrochemical cell as described by Eq. (1). Nevertheless, based on the data presented, it is observed that the potential difference in Fig. 4b and Fig. 5b shifts from approximately  $-80$  mV to  $-160$  mV respectively. A plausible explanation for this difference is that these two experiments were performed on different days at probably different ambient temperatures and there might have been some change in the concentration of potassium ferricyanide, leading to the formation of Prussian blue through oxidation.

In the event where the carbon fibre and the Pt-substrate come into physical contact, the potential difference is zero (Fig. 4b and Fig. 5b). Given this situation, a voltage divider is formed between the potentiometer and the system under investigation, where  $R_1$  corresponds to the resistance between the carbon fibre and the conductive substrate through the electrolyte, and  $R_2$  presents the resistance between the carbon fibre and the conductive substrate when in direct contact. As it is the resistance between two electronic conductors,  $R_2$  holds a negligible value that is almost zero. In such situations, the potential difference is zero and follows the voltage divider formula Eq. (2).

$$V = E \left( \frac{R_2}{R_1 + R_2} \right) \quad (2)$$

Utilizing Eq. (2), it becomes feasible to determine the value of  $R_2$  for each point within the image given the knowledge of  $R_1$ . Such an approach would generate a map of resistance across the surface. The schematic diagram presented in Fig. 3b serves as a simple example of the voltage divider, wherein the resistance  $R_2$  is zero. However, there exist other scenarios where  $R_2$  assumes a non-negligible value, such as in cases involving the presence of oxide layers or anti-corrosive coatings on the active surface. Mapping the resistance of these layers can provide an

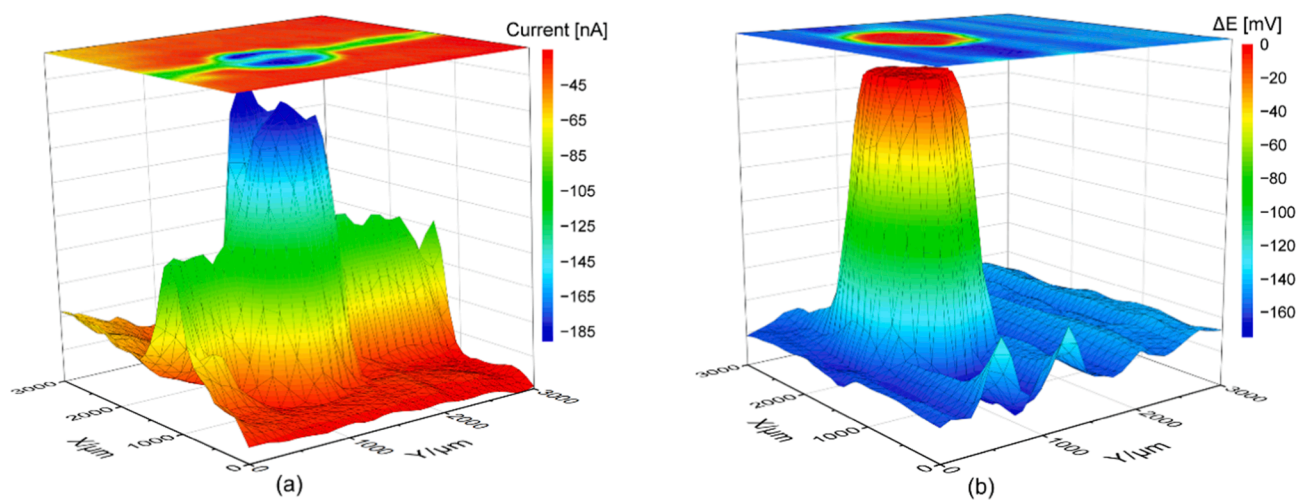


Fig. 5. 3D images of the controlled-cut target obtained by (a) Feedback mode using Pt disk-shaped UME. Current was measured against an Hg/Hg<sub>2</sub>Cl<sub>2</sub>/3M KCl reference electrode. Step size was 100  $\mu$ m on both axes for the Cartesian coordinate-based images. (b) Potentiometric contact-mode using carbon fibre UME. Step size was 100  $\mu$ m on both axes.



insight into their consistency. If the substrate is corroding, an oxide layer is being formed, which could be studied *in situ* in real time. Also, defects in an anti-corrosion layer could be mapped with this technique. These scenarios will be investigated in follow-up papers.

It should be emphasized that the measurements were conducted at room temperature specifically for solid targets. Nevertheless, we anticipate that the measurements could also be conducted on soft surfaces due to the negligible force exerted by the ( $d = 7 \mu\text{m}$ ) carbon fibre. Additionally, any alterations in curvature resulting from temperature changes are expected to be minimal, considering the remarkably low coefficient of thermal expansion of carbon fiber, which is about  $15 \times 10^{-6}/^\circ\text{C}$  [24,25].

Another aspect to highlight is that, due to the curvature of the carbon fibre, the observed potential lags from the actual coordinate of the SECM tip. The alternating scanlines manifest opposing shifts (Fig. 6), necessitating the use of the fast comb algorithm for capturing the 2D images as in Fig. 4 and Fig. 5. Moreover, there exists an asymmetry between the leading and trailing edges of the conductive part of the scanlines. When transitioning from non-conductive to conductive, a sharp potential change to 0 is observed, whereas a clear exponential decay from conductive to non-conductive is seen. This asymmetry arises from the differences in the RC time constants; the conductive region of the image exhibits a low  $R_2$  value, contributing to a lower RC time constant, whereas relatively higher values are present in the non-conductive region.

While the overall performance of the proposed technique can be considered excellent, it is important to acknowledge that there may exist a marginal level of imprecision in the scanning coordinates. In some circumstances, the carbon fibre may manifest a propensity to conform to sudden changes in surface topography resembling the behavior of a phonograph needle, which could result in the exclusion of certain points during the scanning process. The coordinate shifts can be calculated and corrected using geometric arrangements and trigonometric expressions as described by Lesch et al. [19,20].

#### 4. Conclusion

At microscopic scale, surface reactivity of materials can be investigated using the technique called scanning electrochemical microscopy (SECM). Due to the high dependency on sample-tip distance, this method has certain drawbacks when dealing with uneven samples. In this study, a novel approach to resolving this issue using contact-mode carbon fibre electrodes in potentiometric mode was put forth. This approach was applied on a tilted surface and a rough one and compared to the results obtained by the conventional feedback mode. The proposed method demonstrates outstanding efficacy in monitoring sample conductivity irrespective of its topography. Besides being simple and straightforward, the adoption of this technique does not require the use of a reference electrode and utilizes carbon fibre rather than the costly platinum. A limiting factor linked with the suggested methodology involves the induction of a certain degree of inaccuracy in the scanning coordinates, which is correlated with the magnitude of the curvature evident in the carbon fiber.

#### CRedit authorship contribution statement

**Rabea Saleh Rabea Bin Sowad:** Methodology, Formal analysis, Investigation, Writing – original draft, Writing – review & editing, Visualization. **László Kiss:** Methodology, Supervision. **András Kiss:** Conceptualization, Methodology, Software, Resources, Writing – original draft, Writing – review & editing, Supervision.

#### Declaration of Competing Interest

The authors declare the following financial interests/personal relationships which may be considered as potential competing interests:

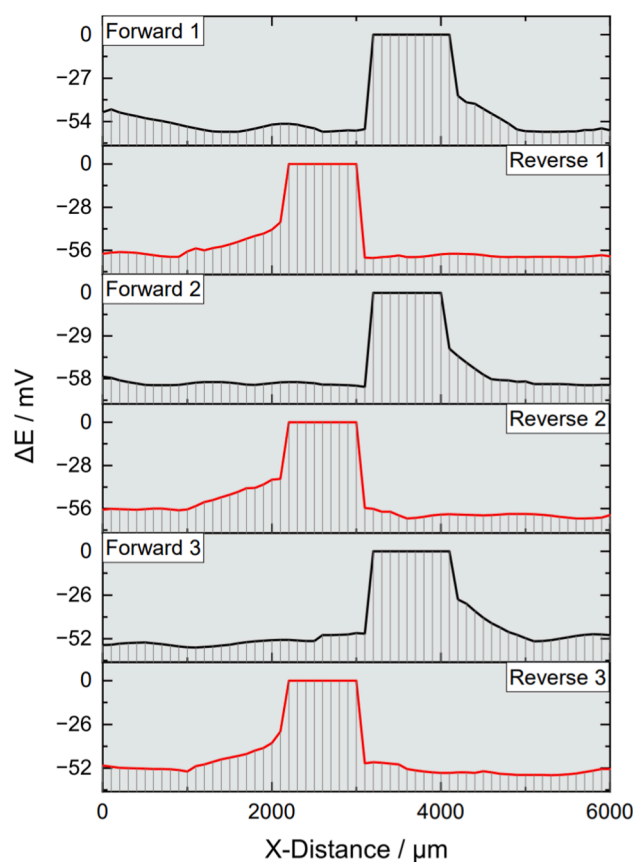


**Fig. 6.** Consecutive alternating scanlines using carbon fibre. The step size was  $100 \mu\text{m}$ , scanning speed was  $1000 \mu\text{m/s}$ . The figure shows the opposing coordinate shift when using alternating scan directions, and the asymmetry of the leading and trailing edge of the conductive part of the image.

[Rabea Bin Sowad Rabea Saleh reports financial support was provided by National Laboratory of Renewable Energies, RRF-2.3.1-21-2022-00009. Andras Kiss reports financial support was provided by National Laboratory of Renewable Energies, RRF-2.3.1-21-2022-00009. Laszlo Kiss reports financial support was provided by Hungarian National Research Development and Innovation Office (NKFI) NKFI-137793. Laszlo Kiss reports financial support was provided by European Social Fund EFOP-3.6.1.-16-2016-00004. Laszlo Kiss reports financial support was provided by The New National Excellence Program of the Ministry for Innovation and Technology Project no. TKP2021-EGA-17.]

#### Data availability

Data will be made available on request.

#### Acknowledgements

This work was supported by the National Laboratory of Renewable Energies, Hungary [RRF-2.3.1-21-2022-00009]; the Hungarian National Research, Development, and Innovation Office [NKFI-137793]; the European Social Fund [EFOP-3.6.1.-16-2016-00004]; the New National Excellence Program of the Ministry for Innovation and Technology [TKP2021-EGA-17]; and the National Research, Development, and Innovation Office [K125244].

#### References

- [1] A.J. Bard, F.R.F. Fan, J. Kwak, O. Lev, Scanning electrochemical microscopy. Introduction and principles, *Anal. Chem.* 61 (2) (1989) 132–138, <https://doi.org/10.1021/ac00177a011>.

- [2] S. Amemiya, A.J. Bard, F.R.F. Fan, M.V. Mirkin, P.R. Unwin, Scanning electrochemical microscopy, *Anal. Chem.* 1 (2008) 95–131, <https://doi.org/10.1146/annurev.anchem.1.031207.112938>.
- [3] F. Cortes-Salazar, D. Momotenko, H.H. Girault, A. Lesch, G. Wittstock, Seeing big with scanning electrochemical microscopy, *Anal. Chem.* 83 (5) (2011) 1493–1499, <https://doi.org/10.1021/ac101931d>.
- [4] D. Polcari, P. Dauphin-Ducharme, J. Mauzeroll, Scanning electrochemical microscopy: a comprehensive review of experimental parameters from 1989 to 2015, *Chem. Rev.* 116 (22) (2016) 13234–13278, <https://doi.org/10.1021/acs.chemrev.6b00067>.
- [5] B. Ballesteros Katemann, A. Schulte, W. Schuhmann, Constant-distance mode scanning electrochemical microscopy (SECM)—part I: Adaptation of a non-optical shear-force-based positioning mode for SECM tips, *Chem.—A European J* 9 (9) (2003) 2025–2033, <https://doi.org/10.1002/chem.200204267>.
- [6] U.M. Tefashe, G. Wittstock, Quantitative characterization of shear force regulation for scanning electrochemical microscopy, *Comptes Rendus Chimie* 16 (1) (2013) 7–14, <https://doi.org/10.1016/j.crci.2012.03.011>.
- [7] H. Shin, P.J. Hesketh, B. Mizaikoff, C. Kranz, Development of wafer-level batch fabrication for combined atomic force-scanning electrochemical microscopy (AFM-SECM) probes, *Sens Actuat B: Chem.* 134 (2) (2008) 488–495, <https://doi.org/10.1016/j.snb.2008.05.039>.
- [8] A.J. Wain, D. Cox, S. Zhou, A. Turnbull, High-aspect ratio needle probes for combined scanning electrochemical microscopy—atomic force microscopy, *Electrochem. Commun.* 13 (1) (2011) 78–81, <https://doi.org/10.1016/j.elecom.2010.11.018>.
- [9] D.J. Comstock, J.W. Elam, M.J. Pellin, M.C. Hersam, Integrated ultramicroelectrode-nanopipet probe for concurrent scanning electrochemical microscopy and scanning ion conductance microscopy, *Anal. Chem.* 82 (4) (2010) 1270–1276, <https://doi.org/10.1021/ac902224q>.
- [10] Y. Takahashi A.I. Shevchuk P. Novak Y. Murakami H. Shiku Y.E. Korchev T. Matsue Simultaneous noncontact topography and electrochemical imaging by SECM/SICM featuring ion current feedback regulation *J. Am. Chem. Soc.* 132 29 2010 10118 10126 10.1021/ja1029478.
- [11] K. Eckhard, W. Schuhmann, Alternating current techniques in scanning electrochemical microscopy (AC-SECM), *Analyst* 133 (11) (2008) 1486–1497, <https://doi.org/10.1039/B806721J>.
- [12] P.M. Diakowski, Z. Ding, Interrogation of living cells using alternating current scanning electrochemical microscopy (AC-SECM), *Phys. Chem. Chem. Phys.* 9 (45) (2007) 5966–5974, <https://doi.org/10.1039/B711448F>.
- [13] M.A. Edwards, A.L. Whitworth, P.R. Unwin, Quantitative analysis and application of tip position modulation-scanning electrochemical microscopy, *Anal. Chem.* 83 (6) (2011) 1977–1984, <https://doi.org/10.1021/ac102680v>.
- [14] M.V. Mirkin, W. Nogala, J. Velmurugan, Y. Wang, Scanning electrochemical microscopy in the 21st century. Update 1: five years after, *Phys. Chem. Chem. Phys.* 13 (48) (2011) 21196–21212, <https://doi.org/10.1039/C1CP22376C>.
- [15] P.M. Diakowski, Z. Ding, Novel strategy for constant-distance imaging using alternating current scanning electrochemical microscopy, *Electrochem. Commun.* 9 (10) (2007) 2617–2621, <https://doi.org/10.1016/j.elecom.2007.08.010>.
- [16] A. Hengstenberg, A. Blöchl, I.D. Dietzel, W. Schuhmann, Spatially resolved detection of neurotransmitter secretion from individual cells by means of scanning electrochemical microscopy, *Angew. Chem. Int. Ed.* 40 (5) (2001) 905–908, [https://doi.org/10.1002/1521-3773\(20010302\)40:5%3C905::AID-ANIE905%3E3.0.CO;2-%23](https://doi.org/10.1002/1521-3773(20010302)40:5%3C905::AID-ANIE905%3E3.0.CO;2-%23).
- [17] Y. Zu, Z. Ding, J. Zhou, Y. Lee, A.J. Bard, Scanning optical microscopy with an electrogenerated chemiluminescent light source at a nanometer tip, *Anal. Chem.* 73 (10) (2001) 2153–2156, <https://doi.org/10.1021/ac001538q>.
- [18] F. Cortés-Salazar, M. Trauble, F. Li, J.M. Busnel, A.-L. Gassner, M. Hojeij, G. Wittstock, H.H. Girault, Soft stylus probes for scanning electrochemical microscopy, *Anal. Chem.* 81 (16) (2009) 6889–6896, <https://doi.org/10.1021/ac900887u>.
- [19] A. Lesch D. Momotenko F. Cortés-Salazar I. Wirth U.M. Tefashe, F. Meiners B. Vaske H.H. Girault G. Wittstock Fabrication of soft gold microelectrode arrays as probes for scanning electrochemical microscopy *J. Electroanal. Chem.* 666 2012 52 61 10.1016/j.jelechem.2011.12.005.
- [20] A. Lesch, D. Momotenko, F. Cortés-Salazar, F. Roelfs, H.H. Girault, G. Wittstock, High-throughput scanning electrochemical microscopy brushing of strongly tilted and curved surfaces, *Electrochim. Acta* 110 (2013) 30–41, <https://doi.org/10.1016/j.electacta.2013.03.101>.
- [21] T. Trenkler, R. Stephenson, P. Jansen, W. Vandervorst, L. Hellemans, New aspects of nanopotentiometry for complementary metal–oxide–semiconductor transistors, *J. Vacuum Sci. Technol. B: Microelectron. Nanometer. Struct. Process. Measur. Phenom.* 18 (1) (2000) 586–594, <https://doi.org/10.1116/1.591237>.
- [22] A. Kiss, G. Nagy, New SECM scanning algorithms for improved potentiometric imaging of circularly symmetric targets, *Electrochimica Acta* 119 (2014) 169–174, <https://doi.org/10.1016/j.electacta.2013.12.041>.
- [23] N. Dang, M. Etienne, A. Walcarius, L. Liu, Scanning gel electrochemical microscopy (SGECM): The potentiometric measurements, *Electrochem. Commun.* 97 (2018) 64–67, <https://doi.org/10.1016/j.elecom.2018.10.020>.
- [24] G. Korb, J. Koráb, G. Groboth, Thermal expansion behaviour of unidirectional carbon-fibre-reinforced copper-matrix composites, *Compos. Part A, Appl. Sci. Manuf.* 29 (12) (1998) 1563–1567, [https://doi.org/10.1016/S1359-835X\(98\)00066-9](https://doi.org/10.1016/S1359-835X(98)00066-9).
- [25] C. Pradere, C. Sauder, Transverse and longitudinal coefficient of thermal expansion of carbon fibers at high temperatures (300–2500 K), *Carbon* 46 (14) (2008) 1874–1884, <https://doi.org/10.1016/j.carbon.2008.07.035>.